UCSF
UC San Francisco Previously Published Works

Title

Metformin and Inhibition of Transforming Growth Factor-Beta Stimulate In Vitro Transport in Primary Renal Tubule Cells

Permalink

https://escholarship.org/uc/item/8wz5b6gx

Journal

Tissue Engineering Part A, 26(19-20)

ISSN

1937-3341

Authors

Love, Harold
Evans, Rachel
Humes, Harvey David
et al.

Publication Date

2020-10-01

DOI

10.1089/ten.tea.2019.0294

Peer reviewed

termis.

Tissue Engineering
& Regenerative Medicine
International Society

ORIGINAL ARTICLE

Metformin and Inhibition of Transforming Growth Factor-Beta Stimulate *In Vitro* Transport in Primary Renal Tubule Cells

Harold Love, PhD,[1] Rachel Evans, BS,[1] Harvey David Humes, MD,[2] Shuvo Roy, PhD,[3] Roy Zent MD, PhD,[1,4] Raymond Harris, MD,[1,4] Matthew Wilson, MD, PhD,[1,4] and William Henry Fissell, MD[1]

Patient-oriented applications of cell culture include cell therapy of organ failure like chronic renal failure. Clinical deployment of a cell-based device for artificial renal replacement requires qualitative and quantitative fidelity of a cultured cell to its *in vivo* counterpart. Active specific apicobasal ion transport reabsorbs 90–99% of the filtered load of salt and water in the kidney. In a bioengineered kidney, tubular transport concentrates wastes and eliminates the need for hemodialysis, but renal tubule cells in culture transport little or no salt and water. We previously identified transforming growth factor-beta as a signaling pathway necessary for *in vitro* differentiation of renal tubule cells. Inhibition of TGF-β receptor-1 led to active inhabitable electrolyte and water transport by primary human renal tubule epithelial cells *in vitro*. Addition of metformin increased transport, in the context of a transient effect on 5′ AMP-activated kinase phosphorylation. The signals that undermine *in vitro* differentiation are complex, but susceptible to pharmacologic intervention. This achievement overcomes a major hurdle limiting the development of a bioreactor of cultured cells for renal replacement therapy that encompasses not only endocrine and metabolic functions but also transport and excretion.

Keywords: renal epithelial cells, NKCC2, TGF-beta, AMPK, metformin

Impact Statement

Clinical tissue engineering requires functional fidelity of the cultured cell to its *in vivo* counterpart, but this has been elusive in renal tissue engineering. Typically, renal tubule cells in culture have a flattened morphology and do not express key transporters essential to their function. In this study, we build on our prior work by using small molecules to modulate pathways affected by substrate elasticity. In doing so, we are able to enhance differentiation of these cells on conventional noncompliant substrates and show transport. These results are fundamentally enabling a new generation of cell-based renal therapies.

Introduction

KIDNEY FAILURE AFFECTS 700,000 Americans and 2 million worldwide. The best and least expensive treatment, transplant, is limited by severe scarcity of donor organs. The vast majority of the half-million Americans with kidney failure are treated with in-center dialysis. For every kidney transplant, 5 people remain on the waitlist and 20 more never have the chance for transplant at all. Dialysis is a recurring expensive, morbid, and burdensome treatment that has been famously said to delay death, but not restore life. The overarching goal of our group is bioengineering a mass-produced universal donor kidney to eliminate the scarcity problem in kidney transplant. In order for this to work, renal tubule epithelial cells in the device must function much like in the *in vivo* kidney niche, which as of yet has been unachievable with regard to transport of salt and water.

Kidneys must excrete a large mass of wastes, while holding the waste concentration in blood at a low value to prevent intoxication. Therefore, a large volume of blood must be processed. In dialysis, even larger volumes of salt water in essence wash the blood. In the kidney, filters called glomeruli separate a large volume (120 L/day) of watery ultrafiltrate from blood and an elaborate gland-like structure

[1]Department of Medicine, Division of Nephrology, Vanderbilt University Medical Center, Nashville, Tennessee, USA.
[2]Internal Medicine, University of Michigan, Ann Arbor, Michigan, USA.
[3]Bioengineering and Therapeutic Sciences, University of California, San Francisco, San Francisco, California, USA.
[4]Department of Medicine, Veterans Affairs Medical Center, Nashville, Tennessee, USA.

called the renal tubule concentrates wastes 100-fold into 1–2 L of urine. Thus, wastes are excreted in fluid volume small enough that it can be balanced by oral intake. Our bioengineering strategy copies the glomerulus-tubule arrangement of the kidney. We pioneered a novel high-efficiency silicon membrane for *in vivo* hemofiltration under the driving force of blood pressure alone, eliminating the pumps wires and power requirements of dialysis.[1–3] A bioreactor of cultured renal tubule epithelial cells uniquely accomplishes two challenging functions. First, the tubule cells use the chemical energy of ATP hydrolysis to selectively reabsorb salt, water, glucose, and amino acids. Second, the cells block reabsorption of uremic toxins. In this way, the bioreactor concentrates wastes in ultrafiltrate to urine without the need for electrical power, pumps, or dialysate.

More broadly, patient-oriented applications of cell culture include organs-on-a-chip devices for drug development and our interest: cell therapy of organ failure. Clinical applications require both qualitative and quantitative fidelity of the cultured cell to its *in vivo* counterpart. A mass-produced device also requires that cells be cultured to differentiated maturity in a manufacturable format. Renal tubular epithelial cells (RTECs) in culture typically assume a flattened morphology lacking the transporters, brush border, and mitochondria needed for transport. We hypothesized that culturing cells on scaffolds that mimicked the elasticity of healthy kidney tissue would promote differentiation. Indeed, primary cells lacked the apical Na+/H+ exchange transporter NHE3 when cultured on stiff substrates, but expressed NHE3 at high levels on soft substrates.[4] By probing molecular pathways perturbed by scaffold stiffness, we identified transforming growth factor-beta (TGF-β) signaling as a potential mediator of the elasticity response.[4] Polyacrylamide hydrogels have poor hydraulic permeability and integrate poorly with standard imaging and measurement tools in cell culture. Therefore, we sought to replicate the effects of scaffold elasticity using pharmacologic manipulation of TGF-β and other metabolic pathways. In an additive manner, TGF-β and metformin increased specific apicobasal transport of salt and water by primary renal tubule cells on conventional easily manufactured cell culture materials, a breakthrough step making achieving an implantable artificial kidney device possible.

Methods

Cell culture

Human renal cortical tubule cells harvested from discarded donor kidneys were purchased from Innovative Biotherapies (Ann Arbor, MI) and were used at 2–3 passage. Cells were seeded onto 1.2 cm^2 permeable supports (Transwell, Corning, Oneonta, NY). All other materials were purchased from Sigma (St. Louis, MO) unless otherwise indicated. Cells were cultured in hormonally defined media as previously described.[4] A small molecule inhibitor of TGF-β inhibitor type 1 (SB431542, 10 μM) and metformin (200 μM) were added to cell culture media. Fluorescein isothiocyanate-conjugated (FITC) inulin (100 μg/mL final concentration) was added in some experiments to evaluate monolayer permeability. Ouabain (10 nM) was added in some experiments to inhibit sodium-potassium ATPase. Cells were grown on a shaker table (73 rpm; equivalent average fluid shear stress 2 dyn/cm^2)

in 95% air, 5% CO_2 at 37°C. Media were changed every 72 h. Volume transport was assessed by weighing media aspirated from apical compartments of the transwells and subtracting from the initial volume. Evaporative controls in the same tray had negligible mass change. As a second estimate of volume change, increase in fluorescence intensity of FITC-inulin was measured and percentage volume change calculated.

Sequential magnetic bead isolation of human proximal tubule cells

Primary human renal epithelial cells (HREC) cells at passage 3 were trypsinized and labeled with biotinylated mouse anti-human CD10 SN5c (Life Technologies; #13-0108-80). CD10-positive cells were isolated with magnetic beads using the CELLection Biotin Binder Kit (Invitrogen; #11533D) according to the manufacturer's instructions. CD10 negative cells were retained and cultured. CD10-positive cells were released from beads and subjected to a second round of selection using biotinylated Anti-Human CD13 (Human Aminopeptidase N, #BAF3815; R&D Systems). CD10-positive/CD13-negative cells were retained and cultured. Double positive CD10/CD13 cells were released from beads and cultured. All cells were plated into six-well Geltrex-coated tissue culture dishes in serum-free HREC medium. Cell viability was >90% throughout.

Western blotting

Cells were rinsed once with phosphate-buffered saline (PBS), then lysed in sodium dodecyl sulfate lysis buffer with protease inhibitor cocktail (Sigma) and phosphatase inhibitors (Roche), and gently scraped from tissue culture plates and collected on ice. Cell suspensions were sheared by passing through a 27G needle, and centrifuged for 10 min at 10,000 *g*. Supernatants were collected and protein was quantified using BCA assays (Pierce). Equal amounts of protein were separated on 4–20% Mini-PROTEAN TGX Precast Gels (Bio-Rad) and transferred to polyvinylidene fluoride membranes (enhanced chemiluminescence [ECL]) or nitrocellulose membranes (Odyssey). Samples were blocked in 5% milk and probed with primary antibody overnight at 4°C. Membranes used with ECL were washed 3 × in Tris-buffered saline with 0.1% Tween 20 (TBST) and incubated in goat anti-rabbit (#W401B; Promega) or goat anti-mouse horseradish peroxidase (#7076P2; Cell Signaling) secondary antibodies (1:2000) for 1 h at room temperature. Membranes were washed 3 × in TBST and developed with Immobilon chemiluminescence substrate (Millipore) and visualized on a Chemi-Doc MP Imaging System (Bio-Rad). For Western blots analyzed using the Li-Cor Odyssey CLx system, nitrocellulose membranes (LI-COR; #92631092) were probed with primary antibodies overnight at 4°C, washed 3 × in TBST, then incubated with donkey anti-mouse IR Dye 800CW, and goat anti-rabbit IR Dye 680RD secondary antibodies at 1:50,000 and 1:20,000 respectively, washed 3 × in TBST, 1 × in TBS (without Tween20), and imaged on Odyssey CLx imaging system (LI-COR Biosciences). Western blot analyses were done using Image Studio 5.2 software (LI-COR Biosciences). Antibodies used were Claudin 2 (#12H12), 1:1000 (Invitrogen), GAPDH (#14C10), 1:5000, NHE3 (#sc-16103), 1:1000 (Santa Cruz),
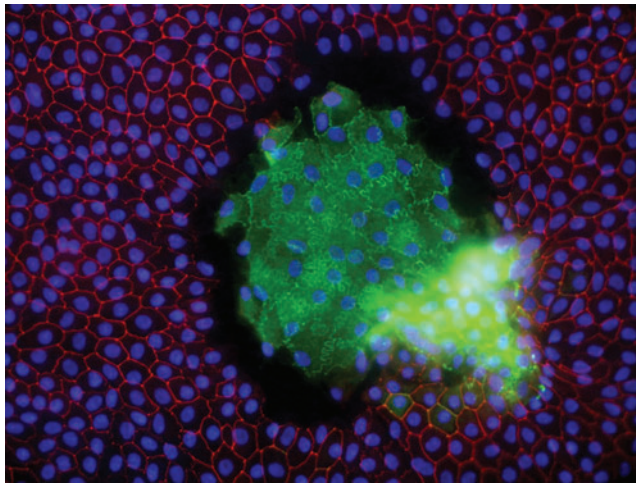
FIG. 1. Segmental origin of cultured cells. Immunofluorescent photomicrograph of cultured primary cells. *Red*, claudin-3, *green*, claudin-2. The vast majority of cells were claudin-3 positive and claudin-2 negative, consistent with origin in the thick ascending limb. Small islands of claudin-2-positive and claudin-3-negative cells were observed, suggesting a scarce population of proximal cells.

sodium–potassium-two-chloride cotransporter 2 (NKCC2; #18970-1-AP), 1:1000 (Proteintech), and pAMPKalpha (cat# 2535S), 1:1000 (Cell Signaling).

Immunofluorescence imaging

Cells were fixed with 4% paraformaldehyde at room temperature. After 5 min of permeabilization with 0.2% Triton-X-100 in PBS followed by 1 h blocking in 10% normal goat serum, proteins of interest were probed with primary antibodies to claudin-2 (Invitrogen; ThermoFisher catalog #32-5600), claudin-3 (Invitrogen; ThermoFisher catalog #34-1700), claudin-7 (SAB4500437; Sigma), ZO-1 Mouse Monoclonal antibody (ZO1-1A12), ThermoFisher (Invitrogen), Cat#33-9100, and NKCC2 (Proteintech; ThermoFisher catalog #18970-1-AP) and visualized with Alexa Fluor 555 or 488 secondary antibodies (Invitrogen) at 1:200 to 1:2000 dilutions. Primary antibodies were incubated overnight at 4°C; secondary antibodies were incubated for 45 min at room temperature. Excess unbound antibody was removed by washing with PBS. 4′,6-Diamidino-2-phenylindole was present in the mounting medium (Vector Laboratory, Burlingame, CA). Fluorescent images were captured on Nikon Microphot FXA or Zeiss Axioskop 2 microscopes paired with Jenoptik ProgRes digital cameras. Images were edited in ImageJ and Adobe Photoshop for false color and to maximize dynamic range. Image intensities in immunohistochemistry images are not quantitative and should not be used to compare abundances within or between images. Renal cells on transwell membranes were stained for NKCC2 and ZO-1 immunofluorescence was also imaged on a Nikon structured illumination microscope (SIM) as a Z-stack at 0.12-μm thickness using a ×100 total internal reflection fluorescence objective. The resulting Z-stack was rendered in three-dimensional in NIS Elements (Nikon) for image analysis. SIM imaging was performed at the Nikon Center of Excellence at Vanderbilt University and the Vanderbilt Cell Imaging Shared Resource.

Electron microscopy

Confluent cells on transwell inserts were rinsed with 0.1 M sodium cacodylate buffer, fixed in 2.5% glutaraldehyde
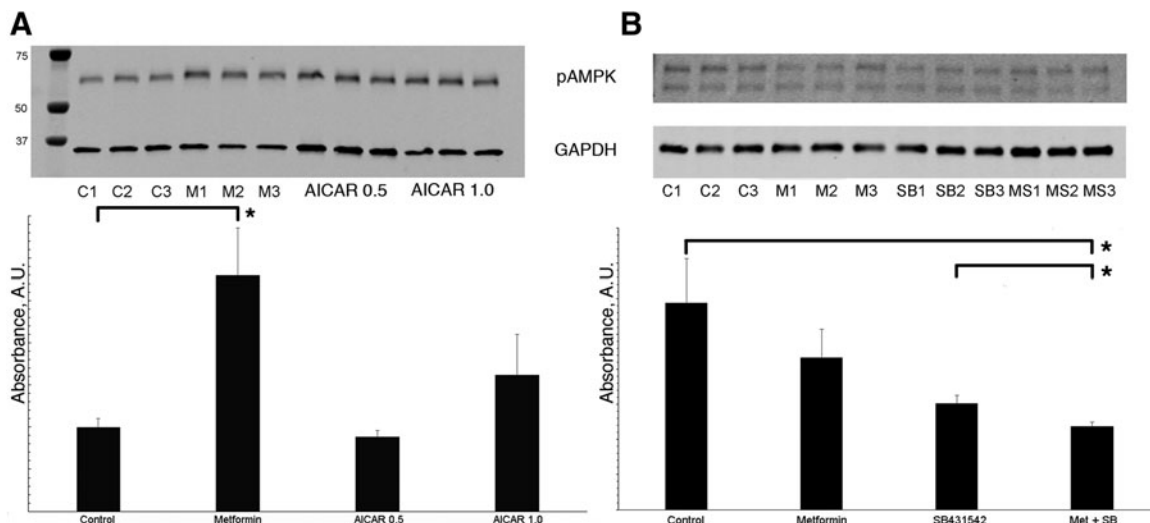
FIG. 2. AMPK phosphorylation is increased by metformin in short-term (8 day) culture, but not long-term (6 week) culture. **(A)** *Top*, Western blot of lysates from primary human renal tubule cells grown on plastic substrates for 8 days; *bottom*, quantification of band density. Cells showed significantly increased AMPK phosphorylation when exposed to 200 μM metformin compared to controls (*$p < 0.05$). AICAR, an AMP mimic, showed a trend toward a dose-dependent effect at 0.5 and 1.0 mM concentration ($p = 0.11$). **(B)** *Top*, Western blot of lysates from primary human renal tubule cells grown on transwells for 6 weeks; quantification of band density. Exposure to SB431542 reduced AMPK phosphorylation with or without metformin ($p = 0.050$ metformin vs. combination and $p < 0.02$ control vs. combination). AICAR, 5-aminoimidazole-4-carboxamide ribonucleotide; AMPK, 5′ AMP-activated kinase.
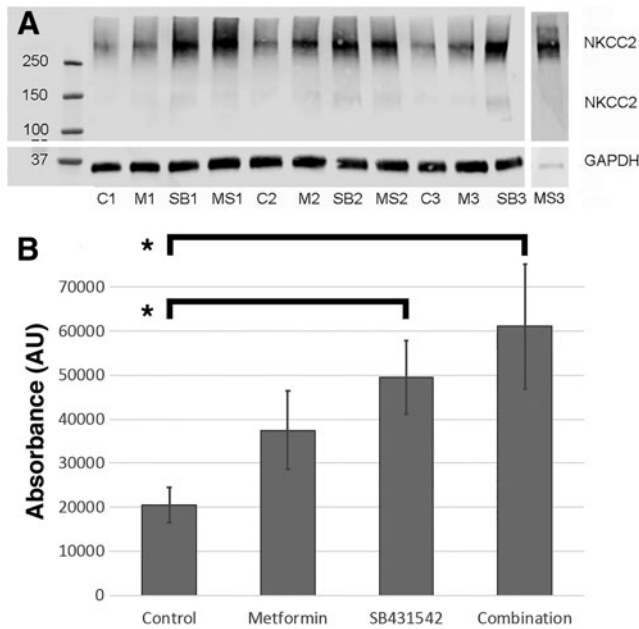
FIG. 3. **(A)** Protein expression of NKCC2 was increased when metformin, SB431542, or combination was added to media. C, control. M, metformin. SB, SB431542; MS, combination. Numbers denote replicates. The *rightmost* band ("MS3") was run on a separate gel due to the limited number of lanes per gel. Despite strong denaturing conditions, we observed a very strong band at about 300 kDa, and a weaker band at about 150 kDa, both of which probed with antibody. We interpret the higher molecular weight bands as NKCC2 dimers as has been reported previously. **(B)** Quantification of Western blot protein expression data by scanning densitometry. $N = 3$ for all experiments. NKCC2 was significantly increased compared to controls in SB431542-treated and combination-treated cells, but not metformin-alone treated cells. *$p < 0.05$. NKCC2, sodium–potassium-two-chloride cotransporter 2.

solution in 0.1 M sodium cacodylate buffer solution for 2 h at room temperature, stored overnight at 4°C, then washed once with 0.1 M sodium cacodylate buffer without glutaraldehyde, and stored at 4°C until submission. For transmission electron microscopy, samples were postfixed with 1.0% os-

mium tetroxide, epoxy embedded, and sectioned to ≈ 70 nm thickness. Sections were poststained with 2.0% uranyl acetate and Reynolds lead citrate. Sections were analyzed and images obtained using a Philips/FEI T-12 Transmission Electron Microscope at an accelerating voltage of 80 kV by an investigator (W.H.F.) blinded to treatment groups. Tissue handling postfixation and image collection was completed at the Vanderbilt Cell Imaging Shared Resource. Mitochondria were counted in five random fields per group by an investigator blinded to treatment allocation.

Statistical analysis

Statistical inference testing for differences between means was performed with Student's t-test without correction for multiple comparisons using Microsoft Excel for Macintosh v 16.16.2.

Results

Primary human renal cortical tubule cells derived from donor kidneys not suitable for transplant[5] at passages 2–3 grew to confluence on Corning Transwell permeable inserts in ~ 10 days ($n = 3$ replicates per condition). Cells remained confluent with stable transepithelial electrical resistance and negligible apicobasal inulin leak rates. An aliquot of cells at passage 3 was sorted by fluorescence-activated cell sorting based on antibodies against CD10 (Common Acute Lymphocytic Leukemia Antigen, a neutral metallopeptidase highly expressed on proximal tubule brush borders). Approximately 1% of cells were CD10+ and the rest were CD10–. Immunofluorescence imaging of cells with antibodies against segment-specific claudins confirmed that only a small minority of cells were derived from proximal segments (Claudin-2 positive), whereas the vast majority were from cortical thick ascending limb (Claudin-3 positive) (Fig. 1). We sought evidence of aquaporin-1 expression by polymerase chain reaction and by Western blot. Consistent with a thick ascending limb origin of the cells, we could not identify any AQP1 expression (data not shown).

Short-term (8 day) addition of 5-aminoimidazole-4-carboxamide ribonucleotide (AICAR) or metformin to cell culture media increased 5' AMP-activated kinase (AMPK)

FIG. 4. Expression of NKCC2. Structured illumination microscopy three-dimensional reconstructions. Primary human renal epithelial cells stained with antibodies against NKCC (*red*) and ZO-1 (*Green*). Nuclei are stained with 4′,6-diamidino-2-phenylindole (*blue*). **(A)** Cross-section. NKCC2 is clearly expressed at the apical membrane surface. **(B)** Perspective rendering from above apical surface showing apical NKCC2 and ZO-1 at the apicolateral margin. **(C)** Perspective rendering from below the basal surface showing apical NKCC2 and ZO-1 at the apicolateral margin.
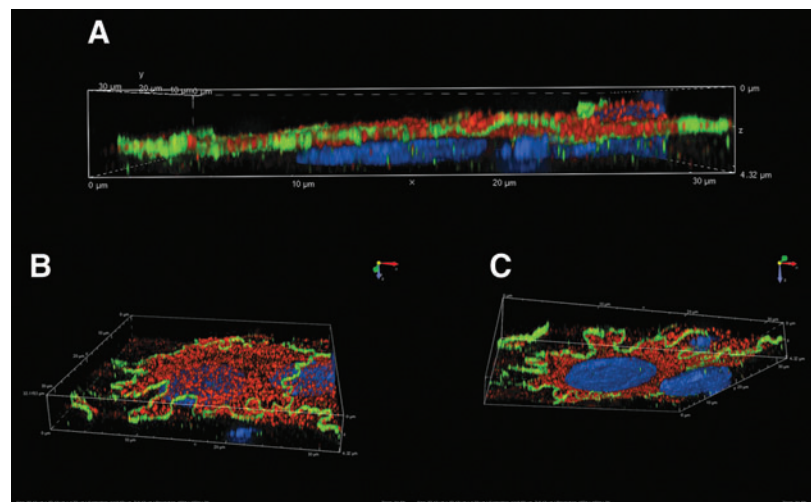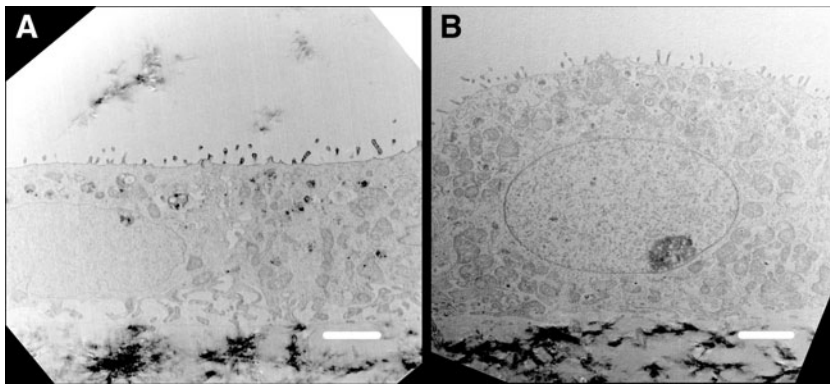
FIG. 5. Transmission electron micrographs of renal tubule cells grown on permeable supports without (**A**) and with (''treated'') (**B**) SB431542 and metformin. Treated cells (**B**) were more cuboidal and less flattened, and had more dense mitochondrial networks ($p = 0.044$ for mitochondrial counts). Apical microvilli were sparse and appeared to be slightly more numerous at the periphery than the center, although the effect was subtle. Scale bar $= 2 \mu m$.

phosphorylation (Fig. 2A). Long-term (6 week) culture of cells on permeable supports did not show increased AMPK phosphorylation in response to metformin (Fig. 2B).

Expression of the NKCC2 was increased in the setting of either metformin, SB431542, or both (Fig. 3), although the increase with metformin alone did not meet statistical significance. All three isolates showed similar NKCC2 expression (data not shown).

Indirect immunofluorescence imaging of cells treated with SB431542 and metformin demonstrated strong apical NKCC2 staining (Fig. 4). We then sought ultrastructural correlates of differentiation in response to TGF-β inhibition and AMPK activation. Transmission electron microscopy of cells grown on Transwells with and without TGF-β inhibitor and metformin showed features consistent with cortical thick ascending limb cells, including sparse brush borders and cuboidal epithelium (Fig. 5).[6] Cells treated with TGF-β inhibitor and metformin had more cuboidal shape and richer mitochondrial networks ($p = 0.044$ for mitochondrial counts).

Our previous experience suggested that prolonged culture was necessary to observe differentiation, so transport was measured on a weekly basis after confluence.[4] At 3 weeks postconfluence, the TGF-β inhibitor SB431542 and metformin were added to media in a 2×2 factorial design. Nine weeks after seeding, we observed dramatically increased apicobasal transport in cells with added TGF-β inhibitor
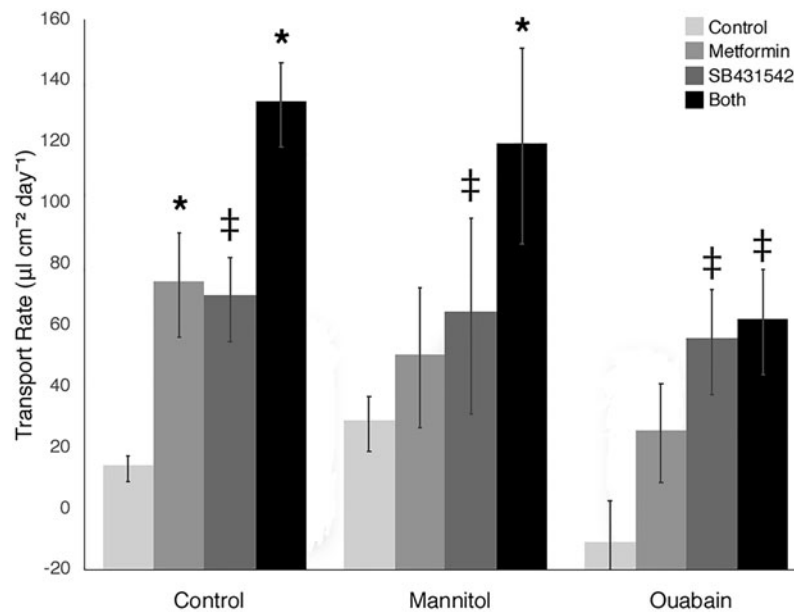

FIG. 6. *In vitro* transport by primary renal tubule epithelial cells. *Left cluster of columns*: cells grown in standard hormonally defined media with added dimethyl sulfoxide transported very small fluid volumes (''Control,'' *pale gray bars*). When metformin (*medium gray bars*) or SB431542, a TGF-βR1 inhibitor (*dark gray bars*), was added to media, transport increased ($p < 0.001$ and $p < 0.02$ vs. control, respectively.) When both metformin and SB431542 were added to media, transport increased further ($p < 0.003$ all comparisons, *black bars*). *Middle cluster of columns*: when mannitol was added to basolateral compartment of the transwells, transport increased slightly in control media, but was unchanged or decreased in cells that received metformin, SB431542, or both, indicating that paracellular apicobasal transport was minimal. *Right cluster of columns*: addition of ouabain (10 nM) significantly decreased transport in all groups. Active transport is seen in primary renal tubule cells allowed to differentiate on permeable supports for 8–10 weeks when metformin, SB431542, or both is added to media. Error bars are standard deviations. *$p < 0.01$ versus controls within each group; ‡$p < 0.05$ versus control within each group. TGF-βR1, transforming growth factor-beta receptor-1.

(4.5-fold increase), added metformin (4.5-fold increase), or both (8.5-fold increase, Fig. 6). TGF-β inhibition and metformin appeared to have independent and additive effects on transport. Monolayer integrity was assessed by inulin leak using FITC-conjugated inulin. The ratio of basolateral to apical fluorescence after 24 h was <0.05 in all cases. Addition of mannitol to the basolateral side of the monolayer increased transport in cells cultured in standard hormonally defined media, but not in cells cultured with added SB431542 or metformin (Fig. 6). Addition of 10 nM ouabain, an inhibitor of basolateral sodium–potassium ATPase, decreased transport without increasing inulin leak (Fig. 6).

We then explored the specificity of transport by probing the effect of an inhibitor of the sodium-proton antiporter NHE3 (tenapanor, 1 μM), the NKCC2 (furosemide, 200 μM), or the sodium-chloride cotransporter NCC (hydrochlorothiazide, 200 μM). Transport was abolished by furosemide ($p < 10^{-3}$) and unchanged by tenapanor or hydrochlorothiazide (Fig. 7). The inulin leak rate was unchanged by the addition of furosemide (Fig. 8).

Taken together, we conclude that transport in these cells is active and dependent on basolateral Na–K-ATPase. Moreover, addition of mannitol did not increase transport, suggesting that transport was primarily transcellular, not passive leakage between cells or through gaps in the monolayer. The minimal amount of paracellular transport is consistent with our observation that these primary cell
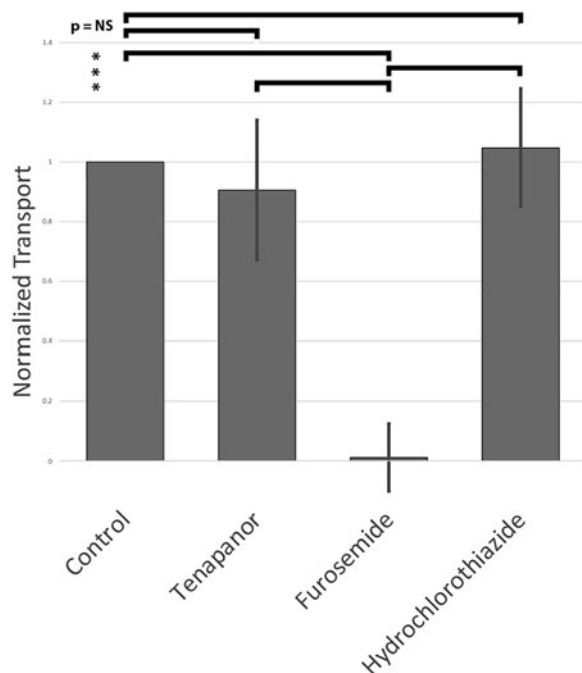
FIG. 7. Diuretic response of cultured primary human renal tubule epithelial cells. Renal tubule epithelial cells were grown to confluence on permeable supports. Fourteen days postconfluence, metformin and SB431542, a TGF-βR1 inhibitor, and each diuretic were added to media. Transport volumes (about 140 μL/cm^2/day) were normalized to volumes in control wells without diuretics. Furosemide abolished transport, while tenapanor and hydrochlorothiazide had no effect. Cultured cells showed specific and inhibitable active apicobasal transport. *$p < 0.05$.
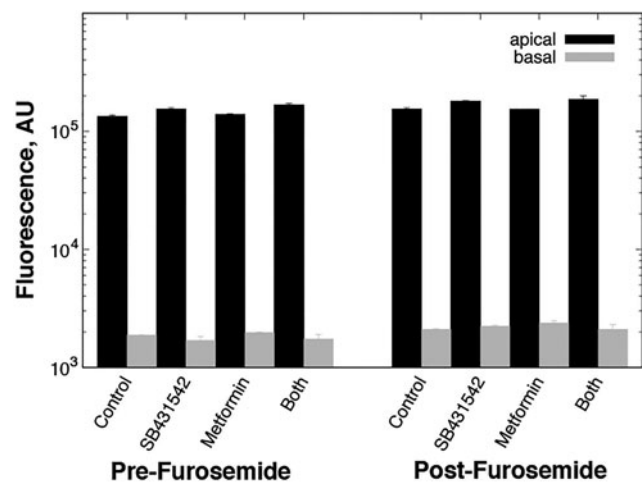
FIG. 8. Inulin leak rates before and after furosemide treatment. Fluorescein isothiocyanate-labeled inulin was added to the apical compartment of each transwell and incubated for ~24 h. After 24 h, fluorescence in the apical and basal media were measured. Data were collected 24 h before incubation with furosemide, and then in the 24 h immediately after the furosemide experiment was complete. Typical ratios of basolateral to apical fluorescence are about 0.01–0.02. In this study, prefurosemide and postfurosemide leak rates are similar and differences did not reach statistical significance by two-tailed Student's t-test. The variation in fluorescence intensity between conditions reflects concentration of the apical media by transcellular transport. Furosemide did not cause paracellular leak.

cultures are a heterogeneous mix of cells, primarily thick ascending limb cells with small numbers of proximal cells as well.

Discussion

To date, active volume transport by cultured primary renal epithelial cells has been elusive. The cell culture techniques used in this study were adapted from pioneering work by Humes et al. and Nowak and Schnellman.[5,7] These primary renal tubule cells have previously been shown to hydroxylate Vitamin D, secrete ammonia in a pH-dependent manner, and transport glucose, confirming the presence of proximal tubule functions.[5] The magnitude of the transport we observed remains ~10-fold lower than Giebisch et al.,[8] measured in freshly isolated rat proximal tubules, or Costanzo and Windhager[9] showed in distal tubules, which may reflect heterogeneity of cells and incomplete optimization of culture conditions.

The cells we have cultured appear to have originated in the thick ascending limb, so comparisons with fresh proximal cells may not be informative. The apparent paucity of cells of proximal segment origin in our low-passage-number culture is intriguing. The cells were derived from the renal cortex and would a priori be expected to contain a preponderance of proximal tubule cells. While different lots of cells from the vendor (Innovative Biotherapies) contained slightly different balances of Claudin-2- and Claudin-3-expressing cells, the trend was consistent that Claudin-3-expressing cells were the most common cell type. Flow

cytometric cell sorting with CD10 and CD13 also showed only 1% of cells at passage 3 were of proximal segment origin. This observation merits further investigation, as it is not yet clear the mechanism by which this selection is occurring, or even if it is happening during initial harvest, during culture, or during passaging.

Modifications to existing culture protocols were motivated by our prior work.[4] First, inhibition of TGF-β pathways has been a part of other advances in renal tubule cell culture models.[10,11] In this study, inhibition of TGF-β receptor-1 with a small molecule was sufficient to enable selective transport, a functional measure of differentiation essential to the identity of the renal tubule cell.

The interdependence of TGF-β and AMPK pathways has been shown previously in renal proximal tubule cells and understood in the context of epithelial-mesenchymal transition.[12] AMPK is phosphorylated at threonine 172 by several enzymes, including TGFβ-activated kinase 1 (TAK1), TGF-β signaling in the kidney is associated with a spectrum of profibrotic functional changes in the nephron, including increased expression of fibronectin, connective tissue growth factor, and collagen I.[12–14] We hypothesized that TGF-β might be involved in the response to substrate elasticity we observed; however, we were surprised that TGF-β inhibition would restore active transport.

AMPK activity has been linked to increased water transport by renal tubule cells in other contexts.[15] AMPK inhibition has been shown to modify cellular response to TGF-β signaling and possibly participate in the causal pathway by which TGF-β causes fibrosis.[12–14] AMPK is a pleiotrophic enzyme that acts on a variety of substrates in response to cues about energy availability in the cell. AMPK itself has multiple regulatory factors, including the tumor suppressor complex LKB1, Stradα, and Mo25; calcium-/calmodulin-dependent protein kinase kinase II, and TAK1. Remarkably, AMPK is associated with passive water transport in the collecting duct as well as transport in more proximal nephron segments. Aquaporin-2 is a vasopressin-regulated water channel in the apical membrane of the principal cells of the collecting duct. Metformin, an activator of AMPK, was associated with increased abundance and phosphorylation of aquaporin-2, although AICAR, an AMP analog that activates AMPK, appeared to prevent aquaporin-2 accumulation in collecting duct cells.[16,17] This suggests that so-called "off-target" effects of metformin that occur in parallel with AMPK activation may be important to tubular transport.

We initially hypothesized that metformin was acting through phosphorylation of AMPK. However, long-term culture and exposure of these cells to metformin had an unanticipated decreasing effect on AMPK phosphorylation. Primary renal tubule cells cultured on permeable supports for 6 weeks showed slightly less AMPK phosphorylation when metformin or SB4315642 was added to media than in controls. We hypothesize that the difference between our findings and the expected increase in AMPK phosphorylation arises from two factors. First, we were unable to locate other references in the literature that examined metformin-AMPK interactions at 6 weeks of cell culture. As cells differentiate, they likely alter cell surface transporters that control drug entry and efflux. Second, we used metformin concentrations about 10-fold lower than the 1–2 mM concentrations reported elsewhere. We chose 200 μM because a dose-ranging study showed toxicity at concentrations above about 500 μM in our cells in our conditions. This concentration is similar to reported plasma concentrations of metformin, but much less than concentrations reported for *in vitro* cell culture.[18] Metformin is a pleiotrophic molecule with multiple mechanisms of action beyond inhibition of mitochondrial complex I. The specific mechanism by which metformin is enabling for differentiation and transport is not yet fully defined and is a subject of further investigation.

The role of culture duration remains enigmatic. We have observed that prolonged culture (25–28 days) appears essential for transporter expression, but we have not conclusively identified explanatory processes *in vitro* that evolve along this time scale.[4] Active volume transport by renal epithelial cells *ex vivo* should have wide-ranging impact on a variety of applications, including pharmacologic, toxicologic, and therapeutic. We have recently used genome engineering technology to improve transport function in renal epithelial cells by overexpression of channels and transporters.[19] Importantly, enhancing salt and water transport through pharmacologic or genetic manipulation should improve reabsorptive capacity in an implantable bioartifical kidney containing functional RTECs.

Disclosure Statement

W.H.F., H.D.H., and S.R. may have rights to certain intellectual property related to the subject matter of the article. W.H.F. and S.R. are founders of Silicon Kidney, LLC. H.D.L., R.E., M.W., R.Z., and R.H. have no disclosures.

Funding Information

References

1. Fissell, W.H., Dubnisheva, A., Eldridge, A.N., Fleischman, A.J., Zydney, A.L., and Roy, S. High-performance silicon nanopore hemofiltration membranes. J Memb Sci **326,** 58, 2009.

2. Kanani, D.M., Fissell, W.H., Roy, S., Dubnisheva, A., Fleischman, A., and Zydney, A.L. Permeability-selectivity analysis for ultrafiltration: effect of pore geometry. J Memb Sci **349**, 405, 2010.

3. Kensinger, C., Karp, S., Kant, R., *et al.* First implantation of silicon nanopore membrane hemofilters. ASAIO J **62**, 491 2016.

4. Love, H.D., Ao, M., Jorgensen, S., *et al.* Substrate elasticity governs differentiation of renal tubule cells in prolonged culture. Tissue Eng Part A **25**, 1013, 2019.

5. Humes, H.D., Mackay, S.M., Funke, A.J., and Buffington, D.A. Tissue engineering of a bioartificial renal tubule assist device: in vitro transport and metabolic characteristics. Kidney Int **55**, 2502, 1999.

6. Verlander, J.W. Normal ultrastructure of the kidney and lower urinary tract. Toxicol Pathol **26**, 1, 1998.

7. Nowak, G., and Schnellmann, R.G. Improved culture conditions stimulate gluconeogenesis in primary cultures of renal proximal tubule cells. Am J Physiol **268**, C1053, 1995.

8. Giebisch, G., Klose, R.M., Malnic, G., Sullivan, W.J., and Windhager, E.E. Sodium movement across single perfused proximal tubules of rat kidneys. J Gen Physiol **47**, 1175, 1964.

9. Costanzo, E.E., and Windhager, L.S. Calcium and sodium transport by the distal convoluted tubule of the rat. Am J Physiol **235**, F492, 1978.

10. Schutgens, F., Rookmaaker, M.B., Margaritis, T., *et al.* Tubuloids derived from human adult kidney and urine for personalized disease modeling. Nat Biotechnol **37**, 303, 2019.

11. Cruz, N.M., Song, X., Czerniecki, S.M., *et al.* Organoid cystogenesis reveals a critical role of microenvironment in human polycystic kidney disease. Nat Mater **16**, 1112, 2017.

12. Thakur, S., Viswanadhapalli, S., Kopp, J.B., *et al.* Activation of AMP-activated protein kinase prevents TGF-β1-induced epithelial-mesenchymal transition and myofibroblast activation. Am J Pathol **185**, 2168, 2015.

13. Krag, S., Østerby, R., Chai, Q., *et al.* TGF-β1-induced glomerular disorder is associated with impaired concentrating ability mimicking primary glomerular disease with renal failure in man. Lab Invest **80**, 1855, 2000.

14. Zuehlke, J., Ebenau, A., Krueger, B., and Goppelt-Struebe, M. Vectorial secretion of CTGF as a cell-type specific response to LPA and TGF-β in human tubular epithelial cells. Cell Commun Signal **10**, 25, 2012.

15. Glosse, P., and Foller, M. AMP-activated protein kinase (AMPK)-dependent regulation of renal transport. Int J Mol Sci **19**, E3481, 2018.

16. Klein, J.D., Wang, Y., Blount, M.A., *et al.* Metformin, an AMPK activator, stimulates the phosphorylation of aquaporin 2 and urea transporter A1 in inner medullary collecting ducts. Am J Physiol Renal Physiol **310,** F1008, 2016.

17. Al-Bataineh, M.M., Li, H., Ohmi, K., *et al.* Activation of the metabolic sensor AMP-activated protein kinase inhibits aquaporin-2 function in kidney principal cells. Am J Physiol Renal Physiol **311,** 890, 2016.

18. Kajbaf, F., De Broe, M.E., and Lalau, J.-D. Therapeutic concentrations of metformin: a systematic review. Clin Pharmacokinet **55,** 439, 2016.

19. Wilson, M.H., Veach, R.A., Luo, W., Welch, R.C., Roy, S., and Fissell, W.H. Genome engineering renal epithelial cells for enhanced volume transport function. Cell Mol Bioeng **13,** 17, 2019.

Address correspondence to:
William Henry Fissell, MD
Internal Medicine
Vanderbilt University Medical Center
2213 Garland Avenue, S3223 MCN
Nashville, TN 37232
USA

E-mail: william.fissell@vumc.org